

See discussions, stats, and author profiles for this publication at: <https://www.researchgate.net/publication/275525373>

Hyperspectral Deep Ultraviolet Autofluorescence of Muscle Fibers Is Affected by Postmortem Changes

ARTICLE in JOURNAL OF AGRICULTURAL AND FOOD CHEMISTRY · APRIL 2015

Impact Factor: 2.91 · DOI: 10.1021/acs.jafc.5b00668 · Source: PubMed

READS

33

6 AUTHORS, INCLUDING:



Annie Venien

French National Institute for Agricultural Rese...

31 PUBLICATIONS 349 CITATIONS

[SEE PROFILE](#)



Frédéric Jamme

SOLEIL synchrotron

84 PUBLICATIONS 539 CITATIONS

[SEE PROFILE](#)



Thierry Astruc

French National Institute for Agricultural Rese...

62 PUBLICATIONS 693 CITATIONS

[SEE PROFILE](#)

Hyperspectral Deep Ultraviolet Autofluorescence of Muscle Fibers Is Affected by Postmortem Changes

Caroline Chagnot,^{†,‡} Annie Vénien,[†] Frédéric Jamme,^{§,||} Matthieu Réfrégiers,^{||} Mickaël Desvaux,[‡] and Thierry Astruc*,[†]

[†]UR370 Qualité des Produits Animaux, and [‡]UR454 Microbiologie, Institut National de la Recherche Agronomique (INRA), F-63122 Saint-Genès Champanelle, France

[§]BP48, Synchrotron SOLEIL, L'Orme des Merisiers, F-91120 Gif-sur-Yvette, France

^{||}UAR1008 CEPIA, Institut National de la Recherche Agronomique (INRA), Rue de la Géraudière, F-44316 Nantes, France

Supporting Information

ABSTRACT: After slaughter, muscle cells undergo biochemical and physicochemical changes that may affect their autofluorescence characteristics. The autofluorescent response of different rat extensor digitorum longus (EDL) and soleus muscle fiber types was investigated by deep ultraviolet (UV) synchrotron microspectroscopy immediately after animal sacrifice and after 24 h of storage in a moist chamber at 20 °C. The glycogen content decreased from 23 to 18 μmol/g of fresh muscle in 24 h postmortem. Following a 275 nm excitation wavelength, the spectral muscle fiber autofluorescence response showed discrimination depending upon postmortem time (t_0 versus $t_{24\text{ h}}$) on both muscles at 346 and 302 nm and, to a lesser extent, at 408 and 325 nm. Taken individually, all fiber types were discriminated but with variable accuracy, with type IIA showing better separation of $t_0/t_{24\text{ h}}$ than other fiber types. These results suggest the usefulness of the autofluorescent response of muscle cells for rapid meat-aging characterization.

KEYWORDS: *rat muscle fibers, postmortem, meat, UV spectroscopy, histology, fiber types*

INTRODUCTION

Meat comes from skeletal muscle, which generally contains different proportions of the four pure myofiber types: type I, type IIA, type IIX, and type IIB. These contain the myosin heavy-chain isoforms (MyHC) I, IIA, IIX, and IIb, respectively.^{1,2} Hybrid fibers intermediate between two pure types and containing two different myosin isoforms (I-IIA, IIA-IIX, and IIX-IIb) are also found. The muscle fibers are characterized by their metabolism (oxidative or glycolytic) and their contraction speed (slow or fast). Type I fibers are slow-twitch fibers, and all type II fibers are fast-twitch fibers. Type I and IIA fibers have an oxidative metabolism, and type IIX and IIB fibers have a glycolytic metabolism.^{1,2}

After slaughter of farm animals, muscle undergoes significant metabolic, physical, structural, and biochemical changes that determine the quality of meat and meat products.^{3,4} After bleeding, the muscle is deprived of oxygen and nutrients. Muscle cells will try to survive by degrading their glycogen stock through anaerobic glycolysis. Lactate accumulation in cells is accompanied by a drop in pH. When the energy reserves are depleted, muscle pH stabilizes at values generally between 5.7 and 6.2, termed the ultimate pH. The kinetics of change in pH is species-dependent, and the time to reach the ultimate pH can range from 2 h in poultry to 24 h in cattle. After this first phase of postmortem changes, additional biochemical changes and significant ultrastructural alterations are observed, related to the improvement of meat quality, especially meat tenderness.^{5,6} The speed of these postmortem changes (also called meat maturation) is dependent upon the species and mostly the metabolic and contractile types of the muscles considered.

Degradation of the myofibrillar structure is faster in white fibers than in red fibers.^{5,7}

Postmortem changes can be assessed by mechanical measurements and biochemical and/or ultrastructural analyses, but these methods are usually destructive and time-consuming. Some authors have exploited the variation in the physical properties of muscles to characterize differences in composition by fluorescence spectroscopy.^{8–10} This highly sensitive method detects fluorophores naturally present in muscle whose properties are very sensitive to changes in their environment. Collagen, tryptophan, tyrosine, or NADH are among the most abundant autofluorescent molecules in muscle.⁸ Several years ago, the autofluorescence of the tryptophan signal following meat sample excitation at 290 nm allowed for a correct discrimination of non-aged from aged meat samples.¹¹ However, the analysis was performed on a macroscopic scale and did not address the metabolic and contractile properties of muscles. The analysis at the cell or even the ultrastructural scale is more difficult because of the low availability fluorescence microscopes that allow for an excitation in the deep ultraviolet (UV), which is relevant for studying biomacromolecules that have a strong absorption in this energy range. Indeed, although spectrometers can often go down to 250 nm, microscopes are usually very limited in this range with either 350 nm cutoff or access to only a limited number of excitation wavelengths.

Received: February 4, 2015

Revised: April 22, 2015

Accepted: April 27, 2015

However, the combination of a microscope with a UV fluorescence spectrometer coupled to synchrotron radiation allows for an excitation range of 200–600 nm that has been used to characterize animal tissues at the ultrastructural level.^{12–15}

Thanks to the availability of these tools, it becomes theoretically possible to detect small changes of the tissue and cells and, therefore, characterize the degree of postmortem change in muscle cells. Our goal was to investigate the autofluorescence changes of individual muscle fibers from rat skeletal muscles stored under anoxia during 24 h regarding their metabolism and ultrastructure changes.

MATERIALS AND METHODS

Animals and Samples. The rat model was chosen because it allows for a better control of rearing and slaughter conditions; it is easy to extract entire muscles and obtain early samples in the laboratory by controlling the best kinetic sampling and temperature conditions.

A total of 24 male Wistar rats aged 5 months and weighing about 500 g were bought from Janvier (Saint-Berthevin, France) and housed at 22 °C under 12 h dark/12 h light cycles with water and food *ad libitum* at an INRA animal facility (Installation Expérimentale de Nutrition, Unité de Nutrition Humaine, INRA Theix, Agreement C 63345.14). Rats were anaesthetized by isoflurane gas and decapitated with a guillotine according to the recommendation of our Regional Ethics Committee (C2E2A 2) and French national legislation (JO 87-848). As no act of pain was performed, because the sampling took place after the death of animals, the experimental project was outside the scope of the European Union Directive 2010/63 and, therefore, did not require ethics review. However, the experimental project was followed by the animal welfare structure integrated in the INRA animal facility installation according to French law (Article JO R. 214-103).

Immediately after death, the lower limbs were severed and dissected under sterile conditions. Extensor digitorum longus (EDL), tibialis anterior, gastrocnemius, and soleus muscles from the right and left hindlegs were extracted from tendon to tendon, avoiding any lesions.

Muscle Postmortem Kinetics. Muscles from three rats were immediately cryofixed post-dissection (10 min after decapitation). For the other 21 rats, muscles were suspended at 20 °C in a sterile moist chamber to prevent drying of the muscle and contamination from microorganisms. Lead ballast was attached at the caudal tendon of each muscle (1.5 g for soleus and EDL and 4.5 g for tibialis and gastrocnemius) to preserve the anatomical muscle length (Figure 1).

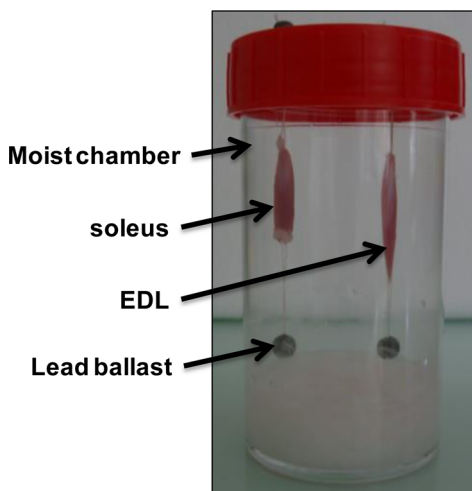


Figure 1. Positioning of the muscles in a moist chamber. Muscles equipped with lead ballast were suspended in a bottle, the bottom of which was lined with a moistened paper towel. The flask was placed in an oven at a temperature maintained at 20 °C.

After 30 min, 1 h, 2 h, 4 h, 8 h, 12 h, and 24 h postmortem, muscles of three rats were removed from their moist chambers and prepared for biochemical and imaging analysis.

pH Measurements. Because EDL and soleus muscles are too small, pH measurements were made on tibialis anterior and gastrocnemius muscles localized around EDL and soleus muscles. pH measurements were made according to the study by Fernandez et al.,¹⁶ adapting to the small quantity of muscle available. Briefly, muscles were weighed and ground in 5 mM idoacetate buffer (2.5 mL/g of muscle), and pH was measured in the muscle suspension at room temperature.

Glycogen Determination. The glycogen content was determined on each right EDL and soleus rat muscle at each time postmortem by enzymatic procedures according to Bergmeyer,¹⁷ with slight modifications. About 0.15 g of muscle tissue was homogenized with 1.8 mL of 0.55 M perchloric acid. On two 0.5 mL aliquots, glycogen was hydrolyzed in glucose with amyloglycosidase. Glucose was converted into 6-phosphogluconolactone after hexokinase and G-6-P dehydrogenase action accompanied by NADH H⁺ production. NADH, proportional to glucose content, was determined by spectrophotometry at 340 nm and compared to standards to calculate the glucose concentration. Results are expressed in micromoles per gram of fresh tissue.

Histology. Cryofixation and Histological Sections. Parts of left EDL and soleus muscles at 0 (t_0) and 24 h ($t_{24\text{ h}}$) postmortem were positioned on a cork plate with embedding medium (Tissue-Tek) and cryofixed by immersion at -160 °C in isopentane cooled with liquid nitrogen (-196 °C). Serial cross-sections of entire muscles (10 μm thick) were cut using a cryostat (Microm, HM 560) and collected on glass slides for histological stains and quartz coverslips for deep UV (DUV) microspectroscopy fluorescence analyses. Sections were stored at -20 °C under vacuum until use. Periodic acid Schiff (PAS) staining was performed for glycogen characterization.¹⁸

Muscle Fiber Type Determination. Fiber types were identified by highlighting the different MyHC using specific mouse monoclonal antibodies BA-D5, SC-71, and BFF3 (AGRO-BIO France). The different primary MyHC antibodies were visualized by an Alexa Fluor 488 labeled goat anti-mouse IgG secondary antibody (A 11001, Invitrogen). In addition, the extracellular matrix (ECM) protein laminin, surrounding the muscle fiber, was stained using an anti-laminin primary polyclonal antibody (L9393 Sigma) and a cyanine-3-labeled secondary antibody (111-165-008, Jackson). The myofiber response to the different MyHC antibodies identified fiber types I, IIA, IIB, and hybrid IIX–IIB. IIX fiber types corresponded to the remaining unmarked cells. Controls were performed with no primary antibody to validate the results.

Image Acquisitions. Observations and image acquisitions were performed using a light microscope (Olympus BX 61) coupled to a high-resolution digital camera (Olympus DP 71) and the Cell F software. PAS-stained sections were examined, and images were acquired in bright-field mode. Immunohistochemistry images were acquired in fluorescence mode (Alexa Fluor 488, 495/519 nm; cyanine 3, 550/570 nm).

Transmission Electron Microscopy. Analysis was conducted on EDL and soleus muscles at 0 and 24 h postmortem from six rats (three rats per postmortem time). Pieces of EDL and soleus muscles of about 4 × 1 mm were fixed overnight at 4 °C by immersion in 2.5% glutaraldehyde in 0.1 M sodium cacodylate buffer at pH 7.2, taking into account muscle fiber direction. Small cubes of about 1 mm³ were post-fixed in 1% osmium tetroxide in 0.1 M sodium cacodylate buffer for 1 h at room temperature. These cubes were dehydrated through a graded ethanol series and embedded in epoxy resin (TAAB, Eurobio France). Ultrathin longitudinal sections (90 nm) (parallel to the fiber direction) were stained with uranyl acetate and lead citrate and examined with a transmission electron microscope (Hitachi HM 7650) using a 80 kV acceleration voltage at the CICS cellular imaging lab on the Clermont-Ferrand University campus (France). Micrographs were acquired with a Hamamatsu AMT digital camera system coupled with the microscope.

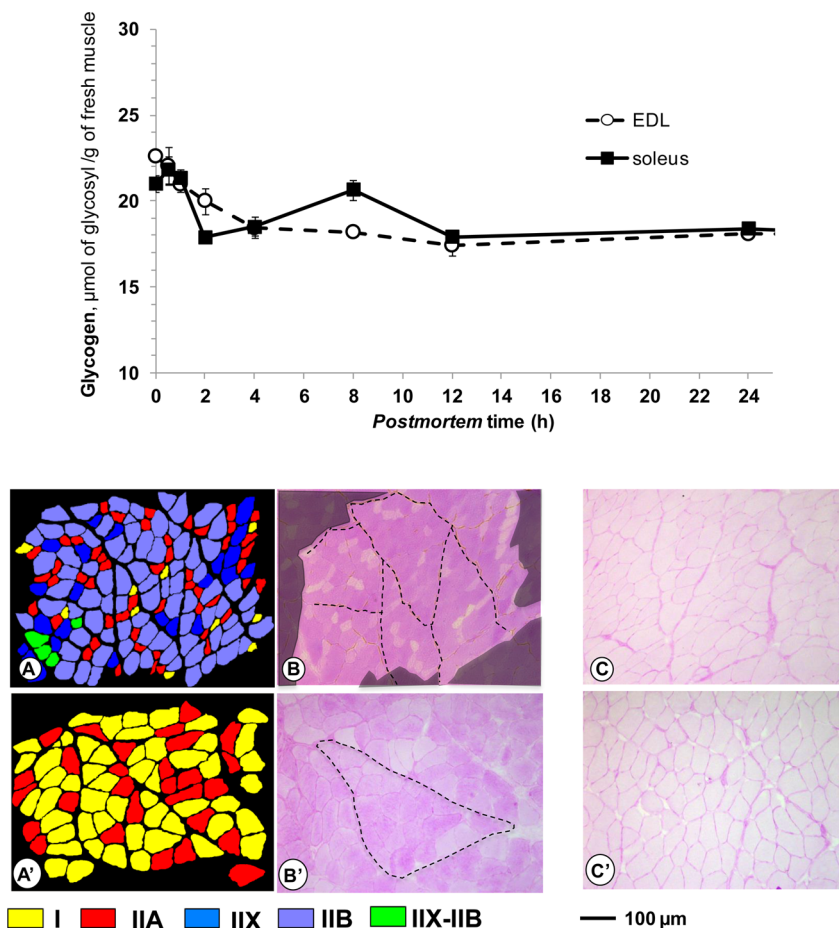


Figure 2. Postmortem evolution of glycogen content in EDL and soleus muscles. The glycogen is degraded in the first hours after slaughter and then stabilizes. Histology revealed the lower glycogen content in oxidative metabolism fibers, particularly in Type IIA fibers. A and A': Fiber type identification of EDL and soleus muscles, respectively. B and B': Glycogen staining of EDL and soleus muscle, respectively, 10 min after animal sacrifice. C and C': Glycogen staining of EDL and soleus muscle, respectively, 24 h after animal sacrifice.

DUV Fluorescence Microspectroscopy. Spotting of Cell Types on Unstained Muscle Serial Cross-Section. From two rat soleus and EDL muscles (0 and 24 h postmortem), an unstained serial section was deposited on quartz coverslips, and using fiber-type identification by immunohistofluorescence on other serial sections, 20 soleus muscle fibers (10 type I and 10 type IIA) and 21 EDL muscle fibers (3 type I, 2 type IIA, 5 type IIX, 8 type IIX–IIB, and 3 type IIB) were spotted for fluorescence spectra acquisition by DUV microspectroscopy.

Spectrum Acquisition. Synchrotron DUV microspectroscopy was performed on the DISCO beamline of the SOLEIL synchrotron radiation facility (Saint-Aubin, France).^{19,20} DUV monochromatized light was used at 275 nm excitation wavelength to excite tissue sections. The emission spectra were acquired from 290 to 540 nm. For each excited pixel, a fluorescence spectrum was recorded. On each spotted cell, 20 acquisitions were made in the intracellular space.

Spectrum Processing and Statistical Analysis. Autofluorescence spectra were spike- and noise-filtered using an in-house program written in MATLAB, version 7.3 (The MathWorks, Natick, MA). The Unscrambler software (version 9.8, Camo Software AS, Norway) was used to perform a baseline adjustment to zero, apply unit vector normalization that normalizes sample-wise the spectral data to unit vectors, and analyze the processed spectra by principal component analysis (PCA). After analysis, the family label of each spectrum was revealed and the two first of the 10 components tested were plotted. The mean spectrum of each group was also plotted for better referencing of the spectral discriminants. Score plots were used to show similarity maps for comparison of spectra, regardless of sample categories. Loading plots derived from the first principal components

(PC1) and second principal components (PC2) were used to reveal and identify characteristic fluorescence peaks.

Numerical variables of fluorescence intensity for wavelengths of interest identified on the PCA loadings were expressed as the mean \pm standard error of the mean (SEM). Variance analysis and mean comparisons were performed using one-way variance analysis and the Student–Newman–Keuls test under the XLSTAT software 2010 (Microsoft Office, Redmond, WA).

RESULTS AND DISCUSSION

Postmortem Metabolism Time Course. The level of EDL and soleus muscle glycogen was about 23 $\mu\text{mol/g}$ of fresh muscle at 10 min postmortem and decreased slightly with time for both muscles (Figure 2). The decrease in contrast of PAS staining with time postmortem reflects a decrease in intracellular glycogen, in agreement with our biochemical data and the literature.^{3,4} However, soon after animal sacrifice, PAS staining intensity depended upon the fiber type. Glycolytic fibers (IIX and IIB) of the EDL were systematically richer in glycogen than oxidative fibers (I and IIA), fully consistent with the literature on the subject.^{3,4} The soleus, which contains only oxidative fibers (I and IIA), also showed a heterogeneous distribution. In this muscle, the IIA fibers contained less glycogen than type I fibers. This result is surprising at first sight because generally IIA fast-twitch fibers have more glycogen reserves than type I slow-twitch fibers to cope with high energy consumption during vigorous exercise. This finding is explained

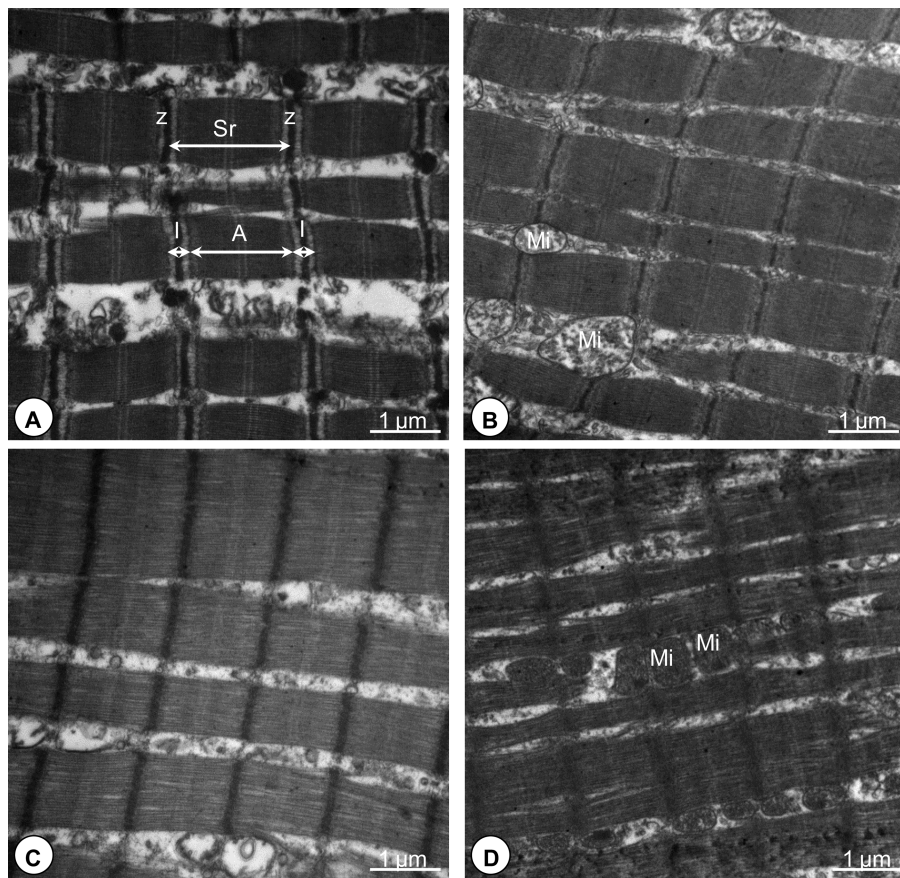


Figure 3. Postmortem ultrastructure changes of EDL and soleus muscles. A, B: EDL muscle at 0 and 24 h postmortem, respectively. C, D: Soleus muscle at 0 and 24 h postmortem, respectively. At slaughter soleus muscle has contracted sarcomeres, which may be the result of cold shortening. The ultrastructure has changed little at 24 h postmortem whatever the considered muscle. Z: Z line, Sr: sarcomere, A: A band, I: I band, Mi: mitochondria.

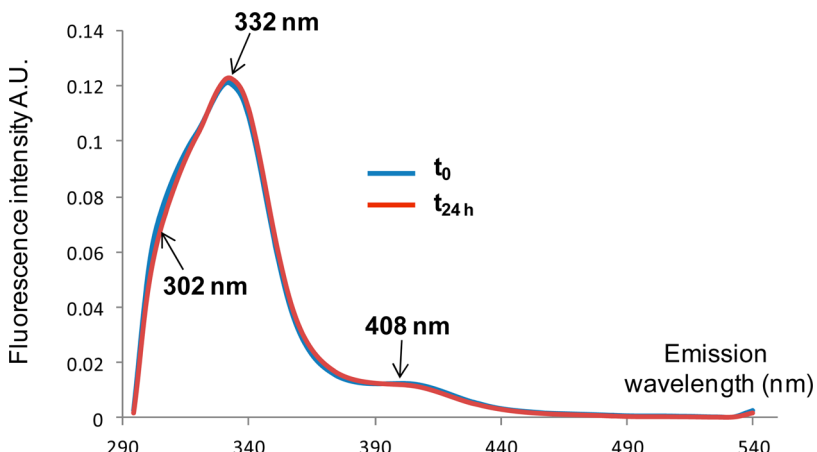


Figure 4. Mean emission fluorescence spectra of 0 (t_0) and 24 h ($t_{24\text{h}}$) postmortem soleus muscle fibers (excitation wavelength of 275 nm). The UV-excited spectra show peaks at 332 nm and 408 nm with shoulders at 302 nm. Fluorescence emission at 302 and 332 are assigned to tyrosine and tryptophan, respectively. Compounds emitting at 408 nm could be NADH. The postmortem time causes a slight shift of the spectrum.

by a specific feature of rodent muscles (rats and mice), whose type IIA fibers are richer in mitochondria and, thus, more oxidative than their type I fibers.^{21,22} It is therefore logical for it to be less richly supplied with glycogen. The initial level of glycogen (around 23 $\mu\text{mol/g}$ of fresh muscle) was lower than reported by others, who found 30–40 $\mu\text{mol/g}$ of fresh muscle in the rat muscle.^{23,24} This difference is probably due to the delay of 10 min necessary for muscle dissection when part of

the glycogen was depleted; 60% of muscle glycogen is degraded within 5 min after the death of the animal.²³ This hypothesis is in accordance with the initial pH (6.9 in tibialis and gastrocnemius muscles), slightly lower than usual *in vivo* pH (7.2), as a consequence of glycogen degradation associated with a release of protons in the tissue.

The rat muscle glycogen content appeared to be considerably lower than seen in farm animal species, where values of

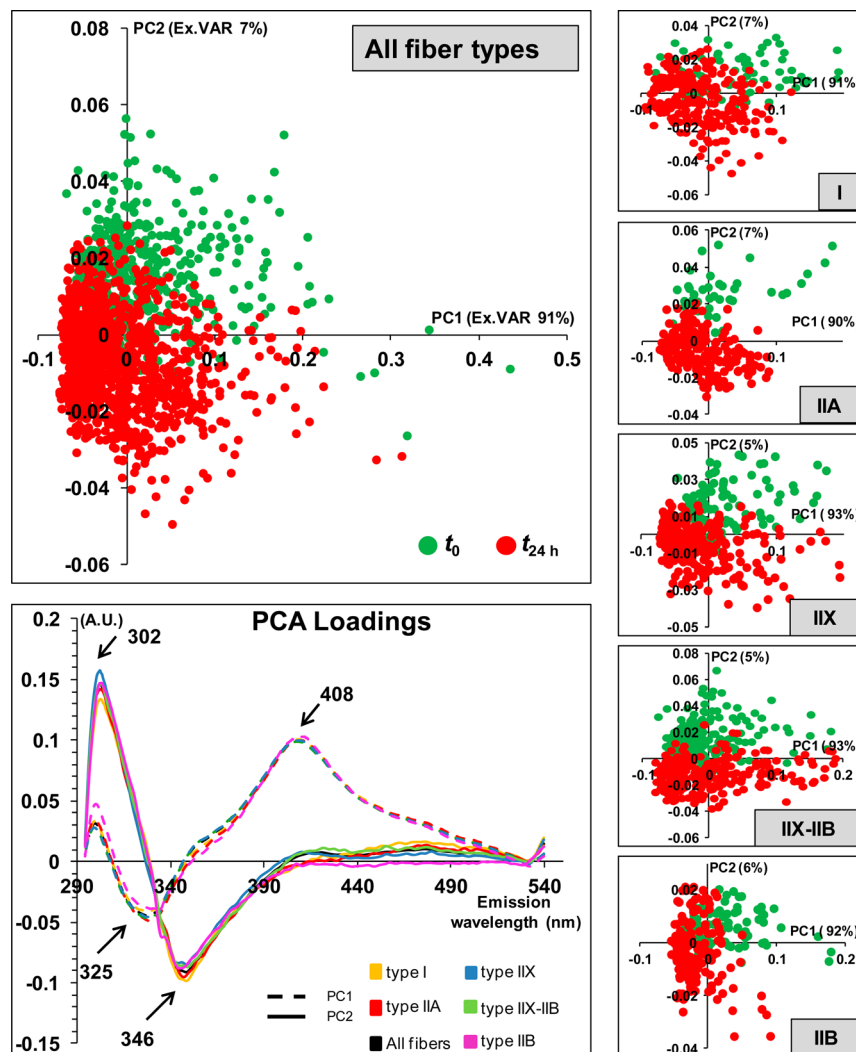


Figure 5. PCA score plots and loadings of fluorescence response of fresh (t_0) and 24 h postmortem ($t_{24\text{ h}}$) EDL muscle. Ex.VAR: explained variance. Postmortem time was most discriminated on the PC2 (346 nm and 302 nm bands) for IIA, IIX, and IIX-IIB fibers and on the PC1 (408 nm and 346 nm bands) for I and IIB fiber types.

glycogen are about 60–70 $\mu\text{mol/g}$ in rabbits,²⁵ 85–100 $\mu\text{mol/g}$ in pigs,^{26,27} 45–50 $\mu\text{mol/g}$ in turkeys,²⁸ 80–100 $\mu\text{mol/g}$ in cattle,^{29,30} and about 70 $\mu\text{mol/g}$ in sheep.³¹ Glycogen reserves remained relatively high in rat muscle (Figure 2), unlike in farm animals, whose meat glycogen reserves fall to less than 10 $\mu\text{mol/g}$ after rigor mortis, with a pH stabilization around 5.6–6.0 depending upon the type of muscle.^{3,4}

The initial pH of the gastrocnemius and tibialis muscle decreased and has reached its minimum (6.06 ± 0.12 and 6.15 ± 0.03 , respectively) after 2.5 h postmortem, which is consistent with the postmortem time of the stopped glycogen consumption in soleus and EDL muscles (Figure 2).

Postmortem Ultrastructural Changes. Representative images of ultrastructural analysis are shown in Figure 3. Shortly after animal sacrifice, the myofibrils were well-preserved with well-defined sarcomeres and aligned Z lines. However, the soleus showed contracted myofibrils that prevented the I bands from being distinguished. This contraction may be related to mechanical stimulation during sampling but also to cold shortening, despite our precautions to avoid this problem (fixative immersion at room temperature). The fact that only the soleus muscle showed this state leads us to believe that it

was due to cold shortening because only red muscles are sensitive to cold shortening.³

After 24 h postmortem, the myofibrils showed no significant change in their structure. Soleus myofibrils were still contracted; however, Z lines remained aligned, and mitochondria were well-preserved, despite the storage temperature of 20 °C, which promotes the action of endogenous proteases.

Appreciable changes were observed at 48 h postmortem on the muscle sample prepared exactly in the same conditions (see Supplementary Figure S1 of the Supporting Information).

Fluorescence Response of Muscle Fibers According to Time Postmortem. Figure 4 shows the profile of fluorescence spectra acquired in soleus muscle fibers at death (t_0) and 24 h postmortem ($t_{24\text{ h}}$) (spectra acquired on the EDL muscle show the same general pattern). The spectra show a peak at 332 nm characteristic of tryptophan and a shoulder at 302 nm assigned to tyrosine.^{12,20,32} The compound that emits fluorescence at 408 nm could not be identified with certainty. Collagen and elastin fluoresce in this wavelength range,¹⁴ but these proteins are located in the ECM, which excludes the involvement of these compounds in the observed fluorescence, because our spectral acquisitions were strictly intracellular. The fluorescence

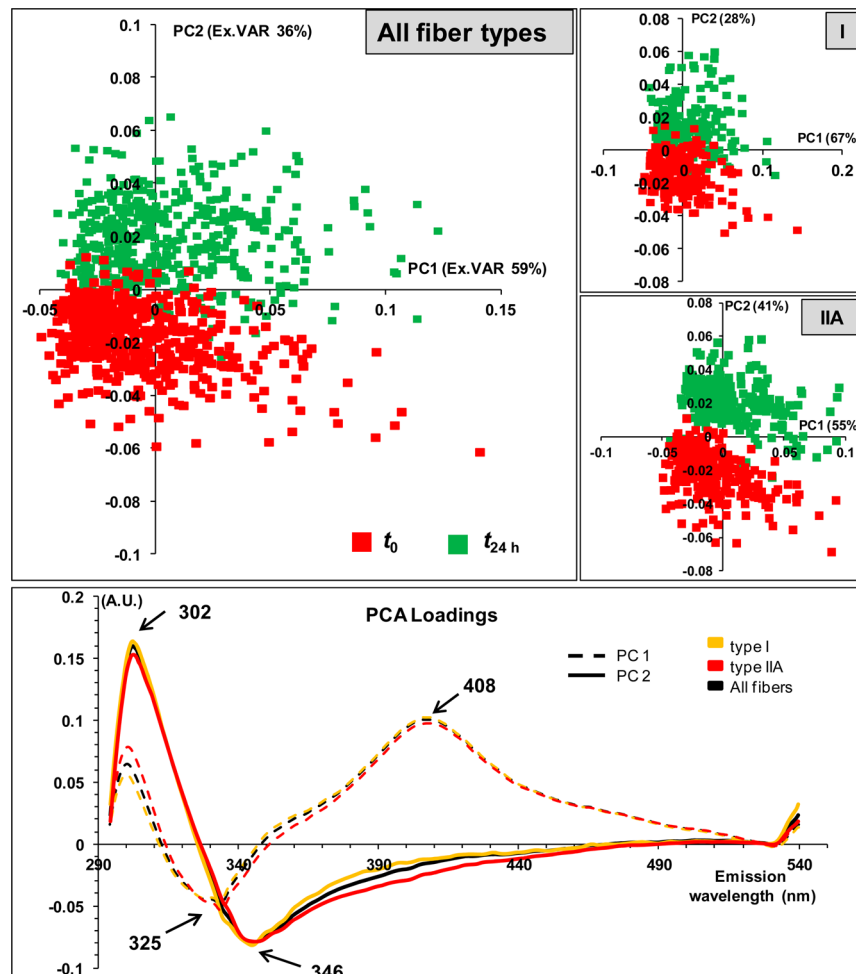


Figure 6. PCA score plots and loadings of fluorescence response of fresh (t_0) and 24 h postmortem ($t_{24\text{ h}}$) soleus muscle. Ex.VAR: explained variance. Postmortem time was best discriminated on the PC2 (346 nm and 302 nm bands) whatever the fiber type of the soleus muscle (I and IIA).

peak at 408 nm could be attributed to NADH, because in living cells, this compound is suspected to fluoresce in this wavelength range.²⁰

The superposition of the spectra acquired at t_0 and $t_{24\text{ h}}$ shows some shifts that are however difficult to see with the naked eye. However, these differences are highlighted by the PCA and variance analysis that are presented in Figures 5–7. PCA and loadings indicate a separation of the two postmortem times (t_0 and $t_{24\text{ h}}$) essentially in the PC2 on the fluorescence intensities at 302 and 346 nm and to a lesser extent on the PC1 at 325 and 408 nm, whichever the muscle considered (Figures 5 and 6). In general, 302 and 408 nm fluorescence intensities were higher and 346 and 325 nm fluorescence intensities were lower for t_0 than for $t_{24\text{ h}}$ samples. Separation on the EDL PCA was less clear-cut than in the soleus, mainly because the EDL is composed of four types of fiber plus IIX–IIB hybrid fibers, while the soleus is composed of only I and IIA fibers.

Some cell types allow for a better separation of postmortem times, such as type IIA fibers, which show excellent discrimination of postmortem times on both the EDL and soleus muscles. IIX–IIB hybrid fibers and IIX fibers (absent in the soleus muscle) also show a good separation with regard to postmortem time. Postmortem time of soleus muscle type I fiber discrimination was somewhat less marked than for type IIA but still very sharp. In contrast, postmortem time discrimination of EDL type I and type IIB fibers was not as

sharp on PC2. For these fiber types, the postmortem time was discriminating on both PC2 at 302 and 346 nm and PC1 at 408 and 325 nm.

Discriminatory wavelengths of PC1 and PC2 were exactly the same for the two muscles (EDL and soleus) and all types of fibers: 325 and 408 nm for PC1 and 302 and 346 for PC2. Hence, it seems that only few fluorophores are concerned in postmortem time discrimination.

Significant differences in emission fluorescence intensities regarding the postmortem time were amplified by the 346/302 and 408/325 ratios, which were systematically lower and higher, respectively, for t_0 than $t_{24\text{ h}}$ muscle fibers (Figure 7). Soleus t_0 fibers I and IIA have a lower 408/325 ratio than EDL t_0 I and IIA fibers (Figure 7). The fluorescence intensity at 408 nm is significantly higher ($p < 0.01$) in the EDL (0.0195 ± 0.0009 and 0.0170 ± 0.0015 for I and IIA fibers, respectively) than in the soleus (0.0114 ± 0.0002 and 0.0113 ± 0.0002 for I and IIA fibers, respectively), while that at 325 nm has very low variations (around 0.110). Therefore, the difference in response is related to the fluorescence emission at 408 nm suspected to correspond to NADH. Moreover, soleus fluorescence at 408 nm is less affected by postmortem time than that of EDL. These results indicate that, within the same type of fiber, the response of some fluorophores may depend upon the muscle origin. Therefore, it seems that the composition or the

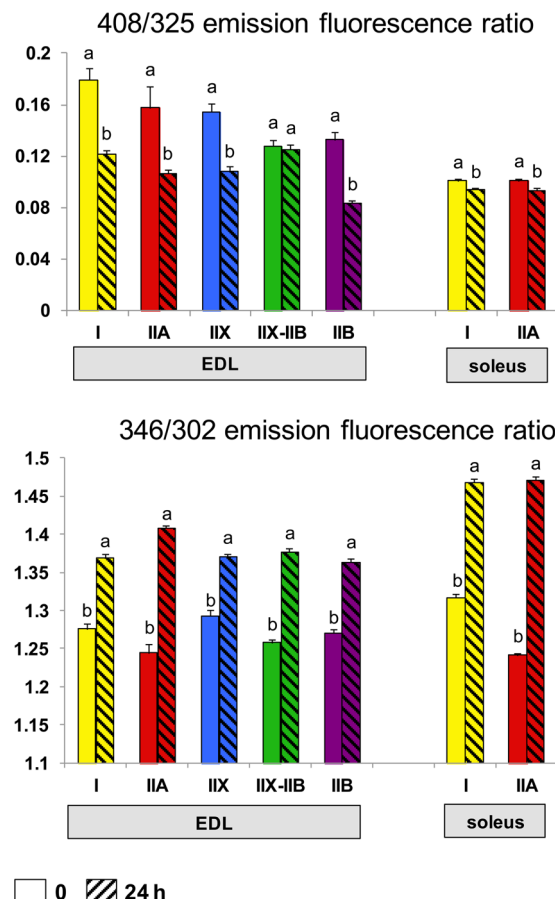


Figure 7. Ratio of fluorescence intensity wavelength evidenced by loadings of PCA regarding the postmortem time. Fluorescence intensity ratio of wavelengths corresponding to discrimination peaks evidenced by PCA allow an amplification of differences. Twenty-four hours postmortem time muscle fibers ($t_{24\text{ h}}$) show higher 346/302 and lower 408/325 values than fresh muscles fibers (t_0). For a given fiber type, different letters indicate a significant difference between 0 and 24 h postmortem samples for $p < 0.01$ (less than 1% that the observed difference is due to coincidence and more than 99% chance that it is related to postmortem time).

intracellular environment of a given fiber type is dependent upon its muscle source.

If the discrimination on 302 and 408 nm is coming from range in fluorescence intensity of tyrosine and NADH, the discrimination on 325 and 346 nm probably originates from slight shifts in the emission fluorescence of tryptophan around 332 nm related to changes in its physicochemical environment.^{33,34} Indeed, after animal slaughter, muscle undergoes structural, biochemical, and physicochemical changes.^{3,4} The pH drop is accompanied by glycogen decrease, lactate accumulation in cells, and muscle contraction. The plasma membranes are quickly perforated,³⁵ and ionic gradients gradually collapse, culminating in ion concentration equilibrium in the cells. Nucleus and organelles (mitochondria, lysosome, sarcoplasmic reticulum, etc.) degrade, and muscle proteins are degraded into peptides under the action of endogenous proteolytic enzymes.^{5,6} All of these phenomena substantially change the intracellular physicochemical environment and, therefore, the fluorescent properties of molecules^{33,34} that may explain the t_0 and $t_{24\text{ h}}$ differences in fluorescence intensity of aromatic amino acids.

The level of discrimination seems dependent upon both muscle (EDL or soleus) and fiber type. In comparison to type I fibers, the better postmortem time separation on IIA fibers suggests more marked environmental changes in these cells.

Postmortem time discrimination being less clear-cut on the EDL than on the soleus muscle is probably related to the fact that the EDL contains four pure types of fibers and IIX–IIB hybrids. In the EDL, the postmortem time of types I, IIB, and IIX fibers was discriminated on both PC1 and PC2, with the $t_{24\text{ h}}$ showing a lower fluorescence intensity at 408 nm and a higher fluorescence at 325 nm than the t_0 .

In comparison to t_0 , the decrease in fluorescence intensity at 408 nm for $t_{24\text{ h}}$ strengthens our hypothesis that this band corresponds to NADH. We know that NADH (fluorescent) is completely oxidized to NAD (non-fluorescent) after a short period of anoxia and all the more so after 24 h postmortem,^{36,37} which would explain the difference in 408 nm intensity as demonstrated on the PC1 loading. The fact that the discrimination at 408 nm was not as clear-cut on some types of fiber may be due to the rate of oxidation of NADH depending upon the fiber type.

Our results demonstrate the benefit of exploiting the variation in DUV autofluorescence feature to characterize some postmortem changes in muscle cells. Despite low spectral differences, multivariate analyzes have identified the wavelengths capable of discriminating muscle samples collected at slaughter from those taken 24 h postmortem. A kinetic study will show whether the evolution of postmortem muscle can be characterized by its autofluorescent answer.

ASSOCIATED CONTENT

Supporting Information

At 48 h postmortem ultrastructure changes in EDL and soleus muscles (Figure S1). The Supporting Information is available free of charge on the ACS Publications website at DOI: 10.1021/acs.jafc.5b00668.

AUTHOR INFORMATION

Corresponding Author

*Telephone: +33-4-73-62-41-56. Fax: +33-4-73-62-42-68. E-mail: thierry.astruc@clermont.inra.fr.

Funding

This work was supported by the French National Institute for Agronomical Research (INRA) with the MICEL project funded by divisions CEPIA and MICA (Science and Process Engineering of Agricultural Products/Microbiology and Food Chain). Caroline Chagnot is a Ph.D. Research Fellow supported by the Région Auvergne (Contrat de Projet État-Région)—FEDER (Fonds Européen de Développement Régional).

Notes

The authors declare no competing financial interest.

ACKNOWLEDGMENTS

Experiments were performed at the SOLEIL synchrotron on the beamline DISCO in the framework of Project 20120364. The authors thank Christophe De l'Homme from the “Installation Expérimentale de Nutrition” (INRA de Theix, Saint-Genès Champanelle, France) for housing rats and technical assistance during animal sacrifice and Claude Ferreira for technical assistance in glycogen determination.

■ REFERENCES

- (1) Astruc, T. Muscle fiber types and meat quality. In *Encyclopedia of Meat Science*, 2nd ed.; Devine, C., Dikeman, M., Eds.; Elsevier: Oxford, U.K., 2014; Vol. 2, pp 442–448.
- (2) Lefaucheur, L. A second look into fibre typing—Relation to meat quality. *Meat Sci.* **2010**, *84*, 257–270.
- (3) Bendall, J. R. Post mortem changes in muscle. In *Structure and Function of Muscle*; Bourne, G. H., Ed.; Academic Press: New York, 1973; pp 243–309.
- (4) Greaser, M. L. Conversion of muscle to meat. In *Muscle as Food*; Bechtel, P., Ed.; Academic Press: New York, 1986.
- (5) Ouali, A. Meat tenderization: Possible causes and mechanisms. A review. *J. Muscle Foods* **1990**, *1*, 129–165.
- (6) Koohmariae, M. Muscle proteinases and meat aging. *Meat Sci.* **1994**, *36*, 93–104.
- (7) Dutson, T. R.; Pearson, A. M.; Merkel, A. A. Ultrastructural postmortem changes in normal and low quality porcine muscle fibers. *J. Food Sci.* **1974**, *39*, 32–37.
- (8) Dufour, E.; Frencia, J. P.; Kane, E. Development of a rapid method based on front-face fluorescence spectroscopy for the monitoring of fish freshness. *Food Res. Int.* **2003**, *36*, 415–423.
- (9) Swatland, H. J. Measurement of the gristle content in beef by macroscopic ultraviolet fluorimetry. *J. Anim. Sci.* **1987**, *65*, 158–164.
- (10) Skjervold, P. O.; Taylor, R. G.; Wold, J. P.; Berge, P.; Abouelkaram, S.; Culoli, J.; Dufour, E. Development of intrinsic fluorescent multispectral imagery specific for fat, connective tissue, and myofibers in meat. *J. Food Sci.* **2003**, *68*, 1161–1168.
- (11) Frencia, J. P.; Thomas, E.; Dufour, E. Measure of meat tenderness using front-face fluorescence spectroscopy. *Sci. Aliments* **2003**, *23*, 142–145.
- (12) Theron, L.; Venien, A.; Jamme, F.; Fernandez, X.; Peyrin, F.; Molette, C.; Dumas, P.; Refregiers, M.; Astruc, T. Protein matrix involved in the lipid retention of foie gras during cooking: A multimodal hyperspectral imaging study. *J. Agric. Food Chem.* **2014**, *62*, 5954–5962.
- (13) Pallu, S.; Rochefort, G. Y.; Jaffre, C.; Refregiers, M.; Maurel, D. B.; Benaitreau, D.; Lespessailles, E.; Jamme, F.; Chappard, C.; Benhamou, C. L. Synchrotron ultraviolet microspectroscopy on rat cortical bone: Involvement of tyrosine and tryptophan in the osteocyte and its environment. *PLoS One* **2012**, *7*, No. e43930.
- (14) Jamme, F.; Kascakova, S.; Villette, S.; Allouche, F.; Pallu, S.; Rouam, V.; Refregiers, M. Deep UV autofluorescence microscopy for cell biology and tissue histology. *Biol. Cell* **2013**, *105*, 277–288.
- (15) Chagnot, C.; Venien, A.; Peyrin, F.; Jamme, F.; Refregiers, M.; Desvaux, M.; Astruc, T. Deep UV excited muscle cell autofluorescence varies with fibre type. *Analyst* **2015**, DOI: 10.1039/C5AN00172B.
- (16) Fernandez, X.; Sante, V.; Baeza, E.; Lebihan-Duval, E.; Berri, C.; Remignon, H.; Babile, R.; Le Pottier, G.; Astruc, T. Effects of the rate of muscle post mortem pH fall on the technological quality of turkey meat. *Br. Poult. Sci.* **2002**, *43*, 245–252.
- (17) Bergmeyer, H. U. *Methods of Enzymatic Analysis*; New York Academic Press: New York, 1974.
- (18) Pearse, A. G. E. *Histochemistry. Theoretical and Applied*, 4th ed.; Churchill Livingstone: Edinburgh, U.K., 1985; Vol. 2.
- (19) Giuliani, A.; Jamme, F.; Rouam, V.; Wien, F.; Giorgetta, J. L.; Lagarde, B.; Chubar, O.; Bac, S.; Yao, I.; Rey, S.; Herbeaux, C.; Marlats, J. L.; Zerbib, D.; Polack, F.; Refregiers, M. DISCO: A low-energy multipurpose beamline at synchrotron SOLEIL. *J. Synchrotron Radiat.* **2009**, *16*, 835–841.
- (20) Jamme, F.; Villette, S.; Giuliani, A.; Rouam, V.; Wien, F.; Lagarde, B.; Refregiers, M. Synchrotron UV fluorescence microscopy uncovers new probes in cells and tissues. *Microsc. Microanal.* **2010**, *16*, 507–514.
- (21) Punkt, K.; Naupert, A.;asmussen, G. Differentiation of rat skeletal muscle fibres during development and ageing. *Acta Histochem.* **2004**, *106*, 145–154.
- (22) Bloemberg, D.; Quadrilatero, J. Rapid determination of myosin heavy chain expression in rat, mouse, and human skeletal muscle using multicolor immunofluorescence analysis. *PLoS One* **2012**, *7*, No. e35273.
- (23) Calder, P. C.; Geddes, R. Post mortem glycogenolysis is a combination of phosphorolysis and hydrolysis. *Int. J. Biochem.* **1990**, *22*, 847–856.
- (24) Manabe, Y.; Gollisch, K. S.; Holton, L.; Kim, Y. B.; Brandauer, J.; Fujii, N. L.; Hirshman, M. F.; Goodyear, L. J. Exercise training-induced adaptations associated with increases in skeletal muscle glycogen content. *FEBS J.* **2013**, *280*, 916–926.
- (25) Astruc, T.; Talmant, A.; Fernandez, X.; Monin, G. Temperature and catecholamine effects on metabolism of perfused isolated rabbit muscle. *Meat Sci.* **2002**, *60*, 287–293.
- (26) Fernandez, X.; Neyraud, E.; Astruc, T.; Sante, V. Effects of halothane genotype and pre-slaughter treatment on pig meat quality. Part 1. Post mortem metabolism, meat quality indicators and sensory traits of m. Longissimus lumborum. *Meat Sci.* **2002**, *62*, 429–437.
- (27) Kocwin-Podsiadla, M.; Przybylski, W.; Kuryl, J.; Talmant, A.; Monin, G. Muscle glycogen level and meat quality in pigs of different halothane genotypes. *Meat Sci.* **1995**, *40*, 121–125.
- (28) Fernandez, X.; Sante, V.; Baeza, E.; Lebihan-Duval, E.; Berri, C.; Remignon, H.; Babile, R.; Le Pottier, G.; Millet, N.; Berge, P.; Astruc, T. Post mortem muscle metabolism and meat quality in three genetic types of turkey. *Br. Poult. Sci.* **2001**, *42*, 462–469.
- (29) McVeigh, J. M.; Tarrant, P. V. Glycogen content and repletion rates in beef muscle, effect of feeding and fasting. *J. Nutr.* **1982**, *112*, 1306–1314.
- (30) Immonen, K.; Ruusunen, M.; Hissa, K.; Puolanne, E. Bovine muscle glycogen concentration in relation to finishing diet, slaughter and ultimate pH. *Meat Sci.* **2000**, *55*, 25–31.
- (31) Diaz, M. T.; Vieira, C.; Perez, C.; Lauzurica, S.; de Chavarri, E. G.; Sanchez, M.; De la Fuente, J. Effect of lairage time (0 h, 3 h, 6 h or 12 h) on glycogen content and meat quality parameters in suckling lambs. *Meat Sci.* **2014**, *96*, 653–660.
- (32) Petit, V. W.; Refregiers, M.; Guettier, C.; Jamme, F.; Sebanayakam, K.; Brunelle, A.; Laprevote, O.; Dumas, P.; Le Naour, F. Multimodal spectroscopy combining time-of-flight-secondary ion mass spectrometry, synchrotron-FT-IR, and synchrotron-UV microspectroscopies on the same tissue section. *Anal. Chem.* **2010**, *82*, 3963–3968.
- (33) Lakowicz, J. R. *Principles of Fluorescence Spectroscopy*, 3rd ed.; Springer: New York, 2006; p 954.
- (34) Valeur, B.; Berberan-Santos, M. N. *Molecular Fluorescence: Principles and Applications*; Wiley-VCH Verlag GmbH: Weinheim, Germany, 2001.
- (35) Astruc, T., Muscle structure and digestive enzyme bioaccessibility to intracellular compartment. In *Food Structure Digestion & Health*, 1st ed.; Boland, M., Golding, M., Singh, H., Eds.; Academic Press: London, U.K., 2014; pp 193–222.
- (36) Ren, J. M.; Henriksson, J.; Katz, A.; Sahlin, K. NADH content in type I and type II human muscle fibres after dynamic exercise. *Biochem. J.* **1988**, *251*, 183–187.
- (37) Mayevsky, A.; Rogatsky, G. G. Mitochondrial function in vivo evaluated by NADH fluorescence: From animal models to human studies. *Am. J. Physiol.: Cell Physiol.* **2007**, *292*, C615–C640.